ADVANCES IN ATMOSPHERIC SCIENCES, VOL. 38, APRIL 2021, 603–614

• **Original Paper** •

Characteristics of Lake Breezes and Their Impacts on Energy and Carbon Fluxes in Mountainous Areas

Lujun XU[1], Huizhi LIU[*1,2], Qun DU[1], Yang LIU[1], Jihua SUN[3], Anlun XU[4], and Xiaoni MENG[1,2]

[1]*State Key Laboratory of Atmospheric Boundary Layer Physics and Atmospheric Chemistry*, *Institute of Atmospheric Physics*, *Chinese Academy of Sciences*, *Beijing* 100029, *China*

[2]*University of Chinese Academy of Sciences*, *Beijing* 100864, *China*

[3]*Yunnan Meteorological Observatory*, *Kunming* 650034, *China*

[4]*Dali National Climatic Observatory*, *Dali* 671003, *China*

(Received 11 September 2020; revised 28 November 2020; accepted 14 December 2020)

ABSTRACT

In mountainous lake areas, lake–land and mountain–valley breezes interact with each other, leading to an "extended lake breeze". These extended lake breezes can regulate and control energy and carbon cycles at different scales. Based on meteorological and turbulent fluxes data from an eddy covariance observation site at Erhai Lake in the Dali Basin, southwest China, characteristics of daytime and nighttime extended lake breezes and their impacts on energy and carbon dioxide exchange in 2015 are investigated. Lake breezes dominate during the daytime while, due to different prevailing circulations at night, there are two types of nighttime breezes. The mountain breeze from the Cangshan Mountain range leads to N1 type nighttime breeze events. When a cyclonic circulation forms and maintains in the southern part of Erhai Lake at night, its northern branch contributes to the formation of N2 type nighttime breeze events. The prevailing wind directions for daytime, N1, and N2 breeze events are southeast, west, and southeast, respectively. Daytime breeze events are more intense than N1 events and weaker than N2 events. During daytime breeze events, the lake breeze decreases the sensible heat flux (Hs) and carbon dioxide flux ($\boldsymbol{F}_{CO_2}$) and increases the latent heat flux (LE). During N1 breeze events, the mountain breeze decreases Hs and LE and increases $\boldsymbol{F}_{CO_2}$. For N2 breeze events, the southeast wind from the lake surface increases Hs and LE and decreases $\boldsymbol{F}_{CO_2}$. Results indicate that lakes in mountainous areas promote latent heat mixing but suppress carbon dioxide exchange.

Key words: sensible heat flux, latent heat flux, carbon dioxide flux, lake breeze, mountain breeze

Citation: Xu, L. J., H. Z. Liu, Q. Du, Y. Liu, J. H. Sun, A. L. Xu, and X. N. Meng, 2021: Characteristics of lake breezes and their impacts on energy and carbon fluxes in mountainous areas. *Adv. Atmos. Sci.*, **38**(4), 603–614, https://doi.org/10.1007/s00376-020-0298-x.

Article Highlights:

- The lake breeze decreases the sensible heat and carbon dioxide fluxes and increases the latent heat flux.
- The mountain breeze decreases the sensible and latent heat fluxes and increases the carbon dioxide flux.

1. Introduction

Nearly 50% of lake area is located in mountainous regions (Verpoorter et al., 2014). The thermal contrast between lake and land drives the formation of lake–land breeze circulation (Bartůňkova et al., 2014; Curry et al., 2015). Thermal contrast forms as slopes heat up (cool down) faster than valleys (Ezber et al., 2015), leading to a pressure-gradient force directed from valley to slope (slope to valley), causing the onset of valley breeze (mountain breeze) circulation (Pérez-Landa et al., 2007b; Ganbat and Baik, 2015). The superimposition of lake–land breeze circulation and mountain–valley breeze circulation leads to an "extended lake breeze" (Kossmann et al., 2002; Zumpfe and Horel, 2007).

The extended lake breeze includes a combination of lake breeze and valley breeze during daytime and a synthesis of land breeze and mountain breeze during nighttime (Kondo, 1990; Laiti et al., 2013a). The intensity of an extended lake breeze usually depends on the extent of the lake, the local topographical features, and the mesoscale systems (McGowan et al., 1995; Gerken et al., 2013; Wagner-Riddle

* Corresponding author: Huizhi LIU
Email: huizhil@mail.iap.ac.cn

© Institute of Atmospheric Physics/Chinese Academy of Sciences, and Science Press and Springer-Verlag GmbH Germany, part of Springer Nature 2021

et al., 2015). In mountainous lake areas, lake and mountain breezes frequently occur under weak synoptic systems (Mahrt, 2017) and are normally characterized by a sudden change in wind speed and direction (Crosman and Horel, 2016; Mahrt, 2017; Wang et al., 2017). Smaller lakes produce weaker and less well-developed extended lake breezes (Boybeyi and Raman, 1992). For lakes with a characteristic dimension larger than 80 km, the extended lake breezes are considered equivalent to sea breezes (Segal et al., 2010). For smaller lakes, the dependence of breeze intensity on the lake's characteristic dimension is low in the late morning but high in the afternoon (Crosman and Horel, 2012).

Extended lake breezes play a significant role in atmospheric boundary layer processes in mountainous lake areas, such as the advection and convection of air flow, exchanges of heat fluxes, and evaporation and precipitation (Sturman et al., 2003; Mengelkamp et al., 2006; Williamson et al., 2009; Serafin et al., 2018). Lakes in mountain basins frequently moisten the air and decrease air temperature in summer (Pu et al., 2016). The lake acts as a source of cold air at the valley bottom, leading to stronger diurnal up-valley wind (Bergström and Juuso, 2006; Laiti et al., 2013b). The interactions between lake and valley breezes could even cause clockwise or anticlockwise circulation, thereby further affecting the mixing of water masses and sedimentation (Hai et al., 2002; Filonov et al., 2015). The extended lake breeze enhances advection of cold air at night, leading to a more stable stratified atmospheric boundary layer in mountainous lake areas (Laiti et al., 2014). On the downwind side, the influence of the extended lake breeze on wind field, temperature, and humidity can be identified nearly as far as 4 km (Bischoff-Gauß et al., 2006). Previous studies have shown that daytime turbulent fluxes over a lake surface can differ from land surface fluxes by up to 200 W m^{-2}, leading to a large thermal contrast between lake and land (Biermann et al., 2014). Lake evaporation accounts for approximately 26% of total evaporation in the Yamdrok Yumtso Lake basin (Xu et al., 2009). According to observation data from the Siling Co Lake on the Tibetan Plateau, temporal variations of evaporation are controlled mainly by the wind speed of the extended lake breeze (Guo et al., 2019). The horizontal and vertical wind associated with the interaction between lake–land and mountain–valley breezes can transport water vapor and pollutants on a large scale (Rotach et al., 2016; Lehner and Rotach, 2018; Tian and Miao, 2019).

Extended lake breezes also play a pivotal role in the transport of carbon dioxide (CO_2) over heterogeneous mountainous lake areas (Lin et al., 2018; Davis et al., 2020; Han et al., 2020). On an interannual scale, lakes serve as a net source of CO_2 to the atmosphere (Borges et al., 2014). The CO_2 flux near the lake surface becomes smaller after sunrise (Du et al., 2018a). Formation of the lake breeze promotes CO_2 flux reduction (Sun et al., 1997). The downslope flow in the mountainous area is usually a positive contributor to CO_2 advection at night, induced by the presence of terrain composed of forest, mosaic trees, and shrubs upwind (Arrillaga et al., 2019). An extended lake breeze can transport CO_2 and airborne pollutants further than "pure" lake or valley breezes could alone (Pérez-Landa et al., 2007a).

So far, characteristics of extended lake breezes and their impacts on energy and carbon fluxes have rarely been analyzed (Nordbo et al., 2011; Alcott et al., 2012; Jeppesen et al., 2016). This lack of statistical features is the major motivation for this study. In addition, most research has focused on case studies occurring over a short period, meaning long-term statistical analyses are still rare (Gerken et al., 2014; Jiménez and Cuxart, 2014). Analysis of these issues has been performed using long-term observation data from an eddy covariance (EC) site at Erhai Lake in the Dali Basin, southwest China. The objectives of this study are to clarify the characterization of daytime and nighttime breeze events in the Dali Basin (an area that includes the Cangshan Mountain range and Erhai Lake) and the effects of these breeze events on energy and carbon fluxes. This paper is organized as follows: the observational site and methodology used to detect breeze events are presented in section 2; Section 3 describes the characteristics of daytime and nighttime breeze events; the effects of breeze events on the sensible heat flux (Hs), latent heat flux (LE), and CO_2 flux ($\boldsymbol{F}_{CO_2}$) exchange are shown in section 4; the main results and conclusions are summarized in section 5.

2. Data and methodology

2.1. *Site and data*

The Dali Basin is located in the Dali Bai Autonomous Prefecture, Yunnan Province, southwest China. The terrain of this basin is high in the northwest and low in the southeast. The average altitude is 2,090 m above sea level (ASL). The Cangshan Mountain range lies in the west of the Dali Basin, running from north to south with 19 peaks. The highest peak is 4,122 m ASL. In the middle of the basin is Erhai Lake (100°05′–100°07′E, 25°35′–25°58′N, 1,972 m ASL), which is 42 km long and 9 km wide on average. The area of Erhai Lake is more than 250 km^2. The average (maximum) depth of the lake is 10 m (20.7 m). The lake is free of ice year-round (Feng et al., 2016). Its water quality is moderately eutrophic. It mainly receives water from 19 streams from the Cangshan Mountains in the west, the Miju River in the north, and the Boluo River in the southeast. The Xier River in the southwest is the only outlet. Land use around the lake is mainly cropland. The Yuan Mountain (2,200 m ASL) is situated to the east of Erhai Lake. In the northeast of the basin is the Jizu Mountain (3,200 m ASL). The basin has extremely complex topography, with large altitude differences and heterogeneous land surfaces (Xu et al., 2016).

The EC observation site is located in Erhai Lake (Fig. 1). It is nearly 80 m from the lake's west shore and 7 km from the east shore. A fixed platform had been established here since June 2011. The EC measurements are complemented by an open-path CO_2/H_2O gas analyzer (LI-7500, LICOR, USA), sonic anemometers (CSAT3A, Campbell, USA), and

Fig. 1. Google Earth image of the study area (left, © Google Earth) and the eddy covariance (EC) observation site (right).

radiation (CNR4, Kipp & Zonen, Netherlands) and photosynthetic active radiation (LI190SB, LICOR, USA) sensors. The EC measurement frequency is 10 Hz. Air temperature, relative humidity (HMP45C, Campbell, USA), wind speed (010C, Campbell, USA) and wind direction are measured at a height of 2 m (020C, Campbell, USA). The 10 Hz raw data were processed using the EddyPro software, Version 6.1. Spikes due to instrument malfunction, weather, and physical noise were removed (Vickers and Mahrt, 1997). A double rotation was applied to align the *x*-axis into the local streamline and turn the vertical wind speed to be zero (Kaimal and Finnigan, 1994). The 30-min Hs, LE and $\boldsymbol{F}_{CO_2}$ were calculated using the eddy covariance method. Corrections for density fluctuations and the frequency losses were made (Webb et al., 1980; Moore, 1986). According to Foken et al. (2004), data quality is classified into three flagging levels (0, 1, and 2). The data marked with flag 2 is abandoned. Overall, 69.8% of Hs, 74.3% of LE, and 76% of $\boldsymbol{F}_{CO_2}$ passed the stationary test. For more measurement details refer to Liu et al. (2015) and Du et al. (2018b).

The variables used in this study were obtained from the EC site and are as follows: wind speed (ws), wind direction (wd), downward solar radiation (K↓), sensible heat flux (Hs), latent heat flux (LE), CO_2 flux ($\boldsymbol{F}_{CO_2}$), and rainfall. The data from 2015 have been unified in 30-min periods, except for the rainfall data which is daily total frequency. Additionally, the ERA-Interim data from the European Centre for Medium-Range Weather Forecasts (ECMWF, https://www.ecmwf.int/en/forecasts/datasets/reanalysis-datasets/era-interim) is analyzed for detecting days with weak synoptic scale processes in 2015. Data at the pixel closest to the EC site is used, with a horizontal resolution of 0.125° every 6 hours. The ERA-Interim data is also used to detect days influenced by cold fronts in 2015. The Dali precipitation data is used to detect days without rainfall.

2.2. *Determination of breeze events*

To analyze the extended lake breezes systematically, daytime and nighttime breeze events are determined according to Arrillaga et al. (2016) and Román-Cascón et al. (2019). The determination of breeze events has four steps, which are as follows:

Step 1: Detect days with weak synoptic scale systems. Days with synoptic wind speed at 700 hPa being lower than 9 m s^{-1} are selected. The ECMWF ERA-Interim data is used to select these days.

Step 2: Detect days without cold fronts. The passage of cold fronts is usually associated with a decrease of equivalent potential temperature. Among days selected in step 1, days with equivalent potential temperature variation at 700 hPa being greater than −1.45 K in 6 hours are retained. The variation of equivalent potential temperature (θ_e) is calculated as follows (Arrillaga et al., 2018):

$$\frac{\Delta\theta_e}{\Delta t} = \frac{\Delta\theta}{\Delta t} + \frac{l_v}{C_{pd}}\frac{\Delta r}{\Delta t},$$

where θ is the potential temperature, $l_v = 2.46\times10^6$ J kg^{-1} is the latent heat of vaporization, $C_{pd} = 1005$ J $kg^{-1}K^{-1}$ is the specific heat at constant pressure for dry air, and r is the water vapor mixing ratio. The potential temperature and water vapor mixing ratio at 700 hPa is obtained from the ECMWF ERA-Interim data.

Step 3: Detect days without precipitation. Among days selected in step 2, days with daily accumulated rainfall being less than 0.5 mm are retained. The daily accumulated rainfall is obtained from the China Meteorological Data Service Center (http://data.cma.cn/).

Step 4: Two additional requirements are needed to detect daytime and nighttime breeze events. One is wind direction in the selected sector, and the other is a minimum persistent duration and dominant frequency of the wind. According to the geographical location of the EC site (Fig. 1), daytime breeze events are determined by wind direction from 0°–170°. Nighttime breeze events at the Dali Basin are affected by the Cangshan Mountain range and Erhai Lake and are therefore usually a combination of mountain breeze and land breeze (Xu et al., 2019). As shown in Fig. 2, nighttime breeze events can be divided into two types. Data shown in Fig. 2 is WRF (The Weather Research and Forecasting Model) simulation data. Model settings are the same as Xu et al. (2019). When the Cangshan Mountain breeze is stronger than the land breeze from the east shore of Erhai Lake, the prevailing wind direction at the EC site is southwesterly, and N1 nighttime breeze events occur (Fig. 2a). Alternatively, when the Cangshan Mountain breeze is weak, the north branch of land breeze circulation in the southern part of the lake reaches midway up its west shore. At that time, the prevailing wind direction at the EC site is southeasterly, and N2 nighttime breeze events occur (Fig. 2b). Wind sectors for N1 and N2 nighttime breeze events are 180°–350° and 90°–170°, respectively. For each breeze event detected, a minimum persistent duration of 3 hours and a frequency of dominant wind direction from the selected sector exceeding 60% are required. The required frequency of dominant wind direction from the selected sector (60%) is different to Román-Cascón et al. (2019) (80%). This is because a standard of 80% may miss the typical lake breeze circulations in summer. Lake breezes in summer usually form 1.5 hours after sunrise and end nearly 1630 LST. The duration of these lake breezes is nearly 8 hours. The EC site (25.77°N, 100.15°E, 2090 m ASL) is located in a low latitude plateau. The sunshine duration is nearly 14 hours (0620~2030 LST) in summer. A criterion of 80% (11.2 hours) is too long and cannot capture daytime breeze events. So in this study, we use a criterion of 60% in the last step.

The number of days meeting the requirements of steps 1–3 was, respectively, 309, 271, and 216. This means that 216 fair-weather days were suitable for the development of breeze events in 2015. The number of daytime breeze events in the Dali Basin was 149 and the number of N1 and N2 events was 22 and 112, respectively.

3. Characteristics of daytime and nighttime breeze events

3.1. *Strength of daytime and nighttime breeze events*

Wind roses for daytime (Fig. 3a), N1 nighttime (Fig. 3b), and N2 nighttime (Fig. 3c) breeze events at the EC site are shown in Fig. 3. During the day, lake breezes typically blow from Erhai Lake to the foot of the Cangshan Mountain range (southeasterly wind). The mean wind direction is 137° with a mean wind speed of 2.78 m s^{-1}. The mean wind direction for nighttime breeze events at the EC site is 236° (N1) and 135° (N2). The N2 breeze events at the EC site are normally more intense than the N1 type (3.06 m s^{-1} vs. 2.17 m s^{-1}). This is partly because the N2 breezes blow from the lake surface, where roughness, and therefore friction, is much less than that of the land surface. Although both the daytime and N2 nighttime breezes blow from the lake surface, the N2 events are more intense. This is due to the fact that the daytime events are mainly lake breezes, while the N2 events are a combination of mountain and land breezes. The

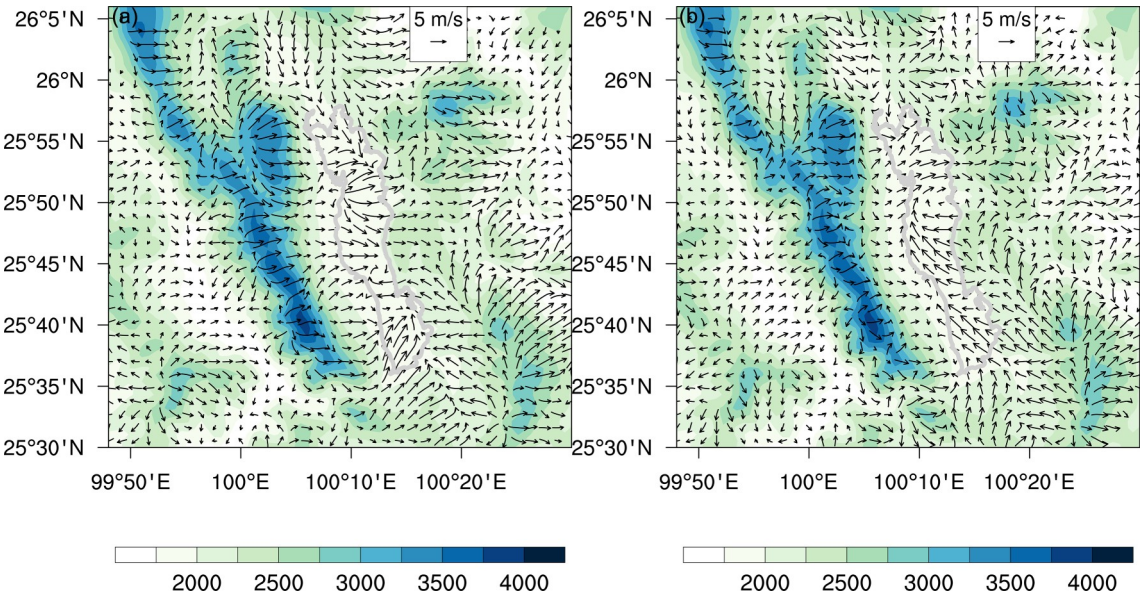

Fig. 2. Wind fields for (a) an N1 nighttime breeze event (02:00 LST 12/08/2015) and (b) an N2 nighttime breeze event (0200 LST 24/10/2015). The gray outline shows Erhai Lake. Shadows indicate altitude (unit: m). Wind vectors and magnitudes are from WRF (The Weather Research and Forecasting Model) simulation data. Model settings are the same as Xu et al. (2019).

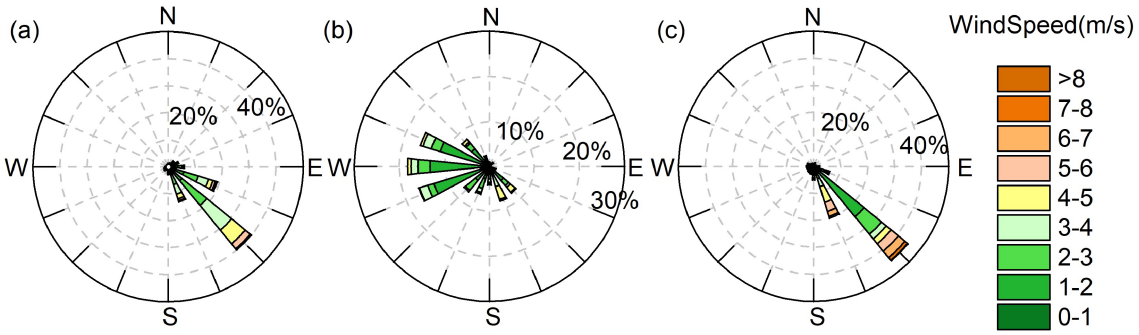

Fig. 3. Wind roses using 30-min averaged data of (a) daytime breeze event, (b) N1 nighttime breeze event, and (c) N2 nighttime breeze event.

southeast wind of N2 breeze events is a branch of the cyclonic circulation in the south of Erhai Lake (Xu and Liu, 2015).

3.2. *Arrival time of daytime and nighttime breeze events*

Figure 4 and 5 show examples of daytime, N1, and N2 breeze events at the EC site. The representative example of the daytime breeze event starts 1.5 hours after sunrise and ends 2 hours before sunset (Fig. 4a). The lake–land breeze circulation dominates daytime breeze events at the Dali Basin. With the formation of the lake breeze after sunrise, wind direction changes from southwesterly to southeasterly and the daytime breeze event starts. At dusk, lake breeze circulation decays and gradually disappears. The downslope flow from the Cangshan Mountain range arrives at the EC site before sunset. Wind direction changes from southeasterly to southwesterly and the daytime breeze event ends. The average daytime breeze event starts at 0830 and ends at 1630

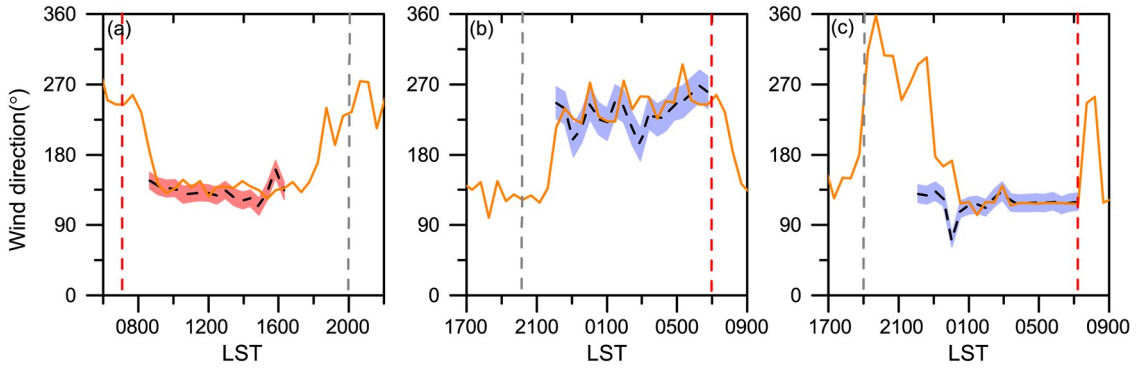

Fig. 4. Wind direction examples for (a) daytime breeze event (11/08/2015), (b) N1 nighttime breeze event (12/08/2015), and (c) N2 nighttime breeze event (24/10/2015) at the EC site are indicated by orange lines. The vertical gray (red) dotted lines indicate sunset (sunrise). The black dots indicate mean wind direction for all events, and the standard deviation is shown with shadow.

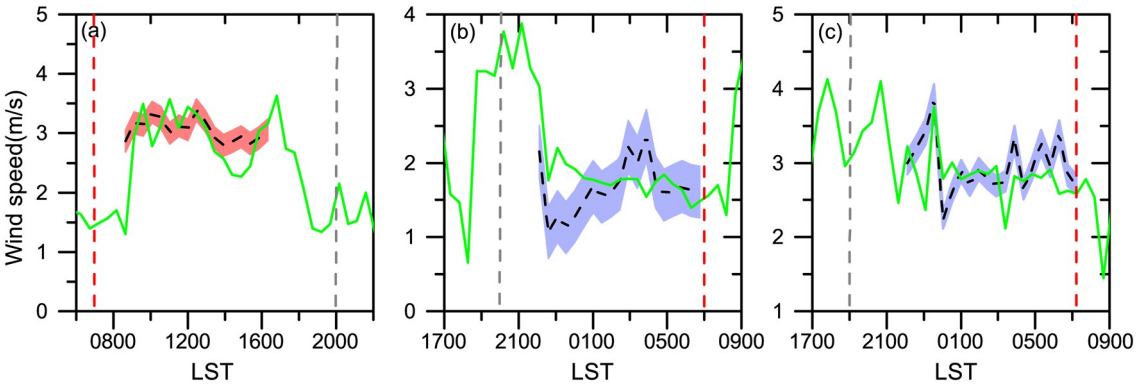

Fig. 5. Wind speed examples for (a) daytime breeze event (11/08/2015), (b) N1 nighttime breeze event (12/08/2015), and (c) N2 nighttime breeze event (24/10/2015) at the EC site are indicated by green lines. The vertical gray (red) dotted lines indicate sunset (sunrise). The black dots indicate mean wind speed for all events, and the standard deviation is shown with shadow.

LST. The average wind direction ranges from 97°–178°.

Mountain breeze circulation dominates the N1 nighttime breeze events. After sunset, mountain breeze circulation forms and develops at the foot of the Cangshan Mountain range. The N1 type breeze event begins 2.5 hours after sunset (Fig. 4b) and maintains until half an hour after sunrise. The average N1 breeze event begins at 2200 and ends at 0630 LST of the following day. The wind direction ranges between 192° and 267° with a standard deviation of nearly 12°. The N2 breeze events are mainly influenced by the land breeze circulation of Erhai Lake and mountain breeze from the Yuan Mountain. A cyclonic circulation forms at the south of Erhai Lake. When its north branch arrives at the EC site, it leads to N2 breeze events. The representative example of an N2 breeze event starts 4 hours after sunset and maintains until sunrise (Fig. 4c). The average beginning time of N2 events is 2200 LST. A southeasterly wind dominates during the entire event. The differences between N1 and N2 events result from the dominating circulation at night. When the mountain breeze from the Cangshan Mountain range is more intense, N1 events may form. When the cyclonic circulation in the southern part of the lake develops and maintains, its northern branch contributes to the formation of N2 events.

At the beginning of daytime breeze events, wind speed increases by nearly 1.3 m s^{-1} (Fig. 5a). The horizontal thermal contrast between lake and land could reach up to 3.5°C (Xu et al., 2019). A large thermal contrast between lake and land leads to a pressure-gradient force, which enhances the wind field (Harris and Kotamarthi, 2005). Roughness of the lake surface is less than land surface, which contributes to the higher wind speed. However, N1 events decrease wind speed from 3 m s^{-1} to nearly 2 m s^{-1} (Fig. 5b). During the afternoon transition, a large thermal difference between mountain slope and valley enhances the strength of the mountain breeze. A sharp decrease appears after that, as the thermal difference becomes smaller. The average wind speed for N1 events ranges from 1.1 m s^{-1} to 2.4 m s^{-1}, which is almost 1.3 m s^{-1} weaker than N2 events. This means that Erhai Lake increases wind speed by at least 1.3 m s^{-1}, which is similar to the results found in southern Manitoba, where the lake breeze increases wind speed by an average 1 m s^{-1} (Curry et al., 2017).

3.3. *Duration of daytime and nighttime breeze events*

The mean duration for daytime, N1, and N2 breeze events is 8, 8.3, and 8.7 hours, respectively (Fig. 6). The duration of each event depends mainly on sunlight hours (Román-Cascón et al., 2019). In general, the lake breeze circulation forms 1–2 hours after sunrise and decays a few hours before sunset. The lake breeze usually arrives at the EC site 1 hour after sunrise (Fig. 7a). This is similar to the Ora del Garda wind in the Italian Alps, for which onset usually

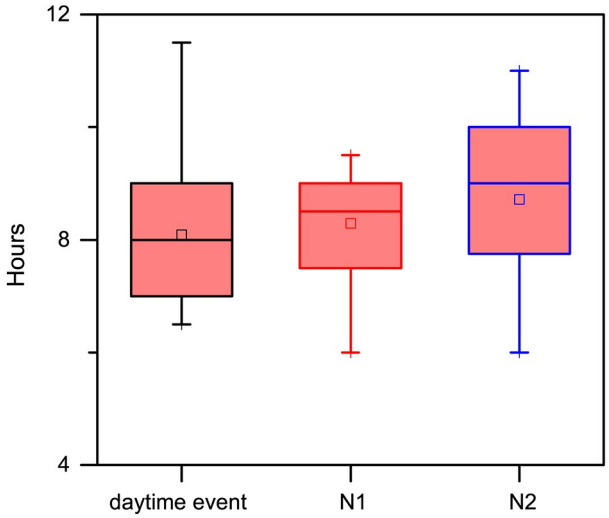

Fig. 6. Duration for daytime, N1, and N2 breeze events. Boxes indicate the central 50% of the distribution, while the upper and lower horizontal lines indicate the maximum and minimum values. The horizontal lines within the boxes indicate the median of the distribution and the small squares indicate the mean value.

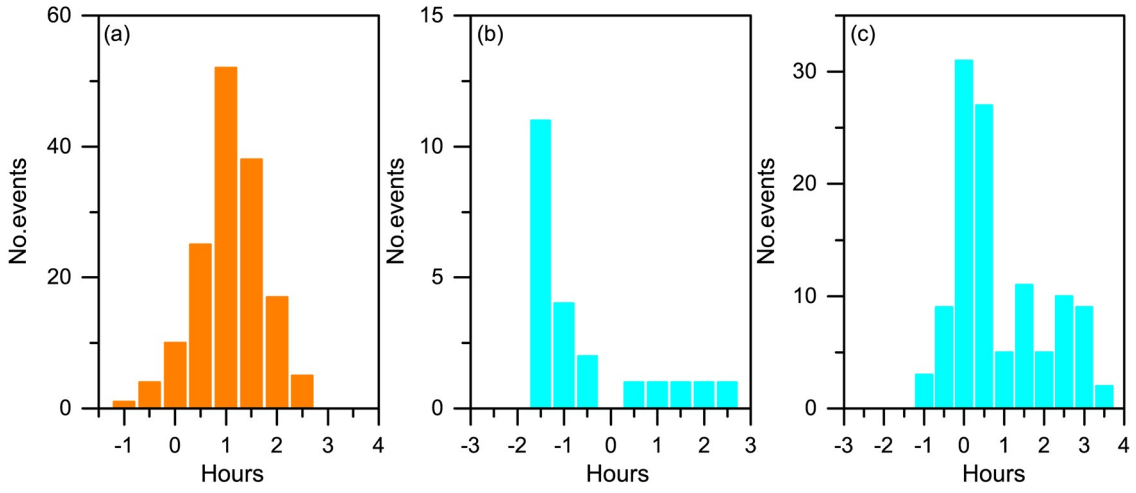

Fig. 7. (a) Number of daytime (in orange) breeze events (*y*-axis) and their arrival time with respect to sunrise; and number of (b) N1 and (c) N2 (in blue) breeze events (*y*-axis) and their arrival time with respect to sunset.

occurs nearly 3 hours after sunrise with cessation around sunset (Giovannini et al., 2015). The mountain breeze from the Cangshan Mountain range usually arrives at the EC site 1.5 hours before sunset (Fig. 7b). As a result, nighttime events persist for longer than daytime events. The N2 events form very close to the time of sunset, although in some cases they can form 2 or 3 hours later (Fig. 7c) depending on the formation of cyclonic circulation at the southern part of the lake. The cyclonic circulation could maintain until sunrise, leading to a longer duration of N2 events compared to the other two types.

4. Impacts of breeze events on energy and carbon dioxide exchange processes

4.1. *Impacts of breeze events on energy fluxes*

The Hs anomalies for daytime, N1, and N2 breeze events are presented in Fig 8. The Hs anomaly is calculated by subtracting the annual average diurnal cycle from the events-mean diurnal cycle of Hs (30-min data) in 2015. The anomalies of representative examples are indicated with green solid lines. The black dotted lines show the average anomaly for each type of event. At the beginning of daytime breeze events at the EC site, the sign of the Hs anomaly changes from positive to negative (Fig. 8a). The arrival of the lake breeze reduces Hs, with the largest negative effect at 0140 LST (6.5 W m^{-2} for event average, 8.2 W m^{-2} in the daytime breeze event example). The N1 events show a larger negative effect on Hs exchange than daytime events (Fig. 8b). After sunset, downslope flow (mountain breeze from the Cangshan Mountain range) brings cold air to the EC site, leading to lower Hs. Moreover, together with the accumulation of colder nocturnal air draining down the slope to the valley, it forms a stable atmospheric boundary layer that weakens turbulent mixing (Fernando et al., 2015). The negative effect of mean N1 events could reduce Hs by an average of 15.1 W m^{-2} at 0100 LST(11.2 W m^{-2} in the N1 event example). However, N2 events increase Hs at night (Fig. 8c). Erhai Lake is warmer than the atmosphere above (Du et al., 2018b), so it transfers heat to warm the atmosphere at night. The southeast wind from the lake surface brings warm air to the EC site, increasing Hs by an average of 12.4 W m^{-2} at 0200 LST (18.7 W m^{-2} at 0130 LST in the N2 event example).

The LE anomalies for daytime, N1, and N2 breeze events are shown in Fig. 9. The LE anomaly is calculated by subtracting the annual average diurnal cycle from the events-mean diurnal cycle of LE (30-min data) in 2015. One hour after sunrise, the LE anomaly changes from negative to positive, and remains positive until sunset (Fig. 9a). The daytime breeze events increase LE by an average of 15.8 W m^{-2}. The lake breeze increases the specific humidity and vapor pressure (Naor et al., 2017). In the representative example of a daytime event, a maximum value of 38.2 W m^{-2} appears at 1200 LST, coinciding with greater wind speed (2.29 m s^{-1}) and vapor pressure difference (increased by 0.16 kPa, Fig. 10a). On average, N1 events decrease LE by 46.6 W m^{-2} at 0230 LST (34.8 W m^{-2} at 0130 LST in the N1 example). The mountain breeze brings dry air to the EC site, resulting in smaller vapor pressure difference (decreased by 0.16 kPa at 0230 LST in the average N1 events, 0.15 kPa at 0130 LST in the N1 example, Fig. 10b) and LE. N2 events increase LE by an average 34.7 W m^{-2}. The average N2 event reaches its largest positive effect of 58.3 W m^{-2} at 0230 LST (59.7 W m^{-2} at 0130 LST in the N2 example). N2 events bring moist air to the EC site, leading to greater vapor pressure difference (increased by 0.39 kPa at 0230 LST on average for N2 events, 0.36 kPa at 0130 LST in the N2 example, Fig. 10c) and enhancement of LE. Although daytime breeze events and N2 nighttime breeze events both increase LE, the positive effect of N2 events is nearly twice as large. This is because wind speed and water vapor pressure difference are greater during N2 events than during daytime events.

4.2. *Impacts of breeze events on carbon dioxide flux*

The F_{CO_2} anomalies for daytime, N1, and N2 breeze

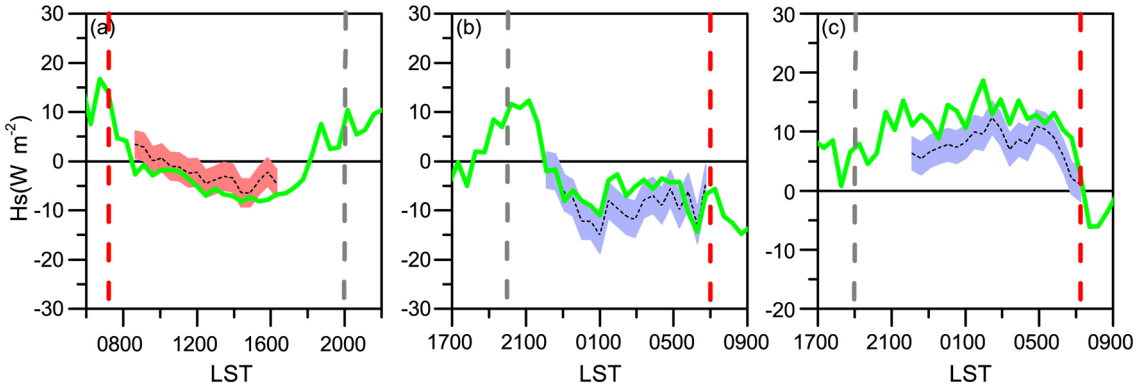

Fig. 8. Hs anomalies for (a) an example daytime breeze event (11/08/2015), (b) an example N1 breeze event (12/08/2015), and (c) an example N2 breeze event (24/10/2015) at the EC site are indicated with green lines. The vertical gray (red) solid lines indicate sunset (sunrise). The Hs anomaly mean for all events is shown with black dots, and the standard deviation is shown with shadow.

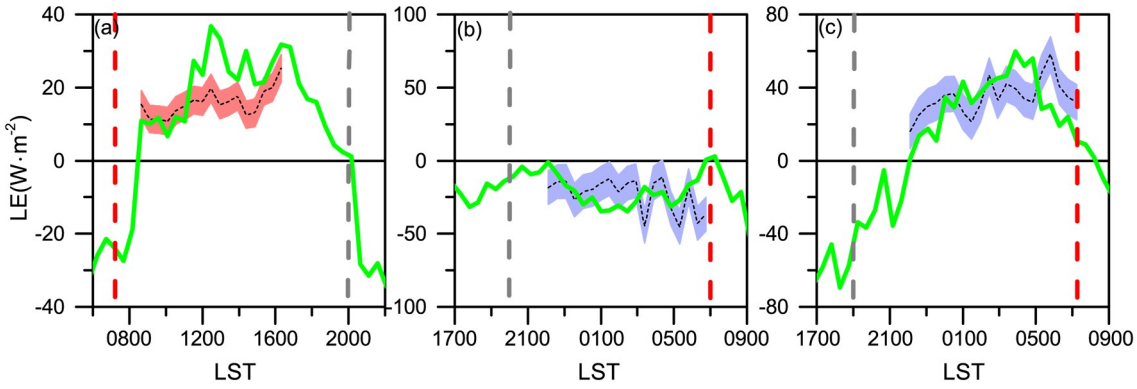

Fig. 9. LE anomalies for (a) an example daytime breeze event (11/08/2015), (b) an example N1 breeze event (12/08/2015), and (c) an example N2 breeze event (24/10/2015) at the EC site are indicated with green lines. The vertical gray (red) solid lines indicate sunset (sunrise). The LE anomaly mean for all events is shown with black dots, and the standard deviation is shown with shadow.

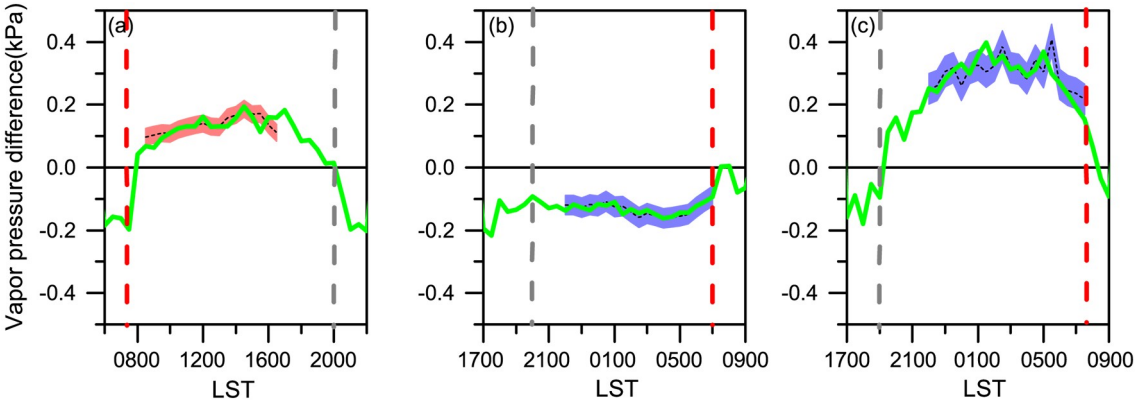

Fig. 10. Vapor pressure difference (e_s–e_a) anomalies for (a) an example daytime breeze event (11/08/2015), (b) an example N1 breeze event (12/08/2015), and (c) an example N2 breeze event (24/10/2015) at the EC site are indicated with green lines. The vertical gray (red) solid lines indicate sunset (sunrise). The vapor pressure difference anomaly mean for all events is shown with black dots, and the standard deviation is shown with shadow.

events are presented in Fig. 11. The $\boldsymbol{F}_{CO_2}$ anomaly is calculated by subtracting the annual average diurnal cycle from the events-mean diurnal cycle of $\boldsymbol{F}_{CO_2}$ (30-min data) in 2015. Both the events-mean and the example given show a similar tendency during daytime events at the EC site, with the $\boldsymbol{F}_{CO_2}$ anomaly changing to negative and remaining negative throughout the day (Fig. 11a). The $\boldsymbol{F}_{CO_2}$ decreases by nearly 0.4 μ mol m^{-2} s^{-1} on average. Aquatic vegetation covers approximately 8% of the lake area, with an average biomass of 12.5 kg (FW) m^{-2} (Li et al., 2011). During the day, aquatic vegetation absorbs CO_2 through photosynthesis, leading to a lower $\boldsymbol{F}_{CO_2}$ around the lake surface. Meanwhile, the lake increases local wind speed, which also has a negative impact on $\boldsymbol{F}_{CO_2}$ on the diurnal scale (Du et al., 2018a).

Associated with the formation of nighttime mountain-breeze circulation, the mean N1 events increase $\boldsymbol{F}_{CO_2}$ by 2.1 μ mol m^{-2} s^{-1}. At night, respiration of vegetation absorbs O_2 and releases CO_2, which increases $\boldsymbol{F}_{CO_2}$. The $\boldsymbol{F}_{CO_2}$ is higher in mountain areas than it is at the lake surface, so the mountain breeze increases $\boldsymbol{F}_{CO_2}$ at the EC site. Influenced by the southeast wind from the lake surface, the mean N2 events decrease $\boldsymbol{F}_{CO_2}$ by 1.8 μ mol m^{-2} s^{-1}. The warm lake surface leads to a higher atmospheric boundary layer over water than over land at night (Xu et al., 2019), which contributes to the lower $\boldsymbol{F}_{CO_2}$ above the lake surface. Different types of breeze events thus affect the $\boldsymbol{F}_{CO_2}$ in different ways. Mountain breezes increase $\boldsymbol{F}_{CO_2}$, while lake breezes decrease $\boldsymbol{F}_{CO_2}$. On the annual scale, daytime, N1, and N2 nighttime breeze events contribute −8.22%, −6.64%, and 12.84% to Hs, respectively. The contribution rates of daytime, N1, and N2 nighttime breeze events on LE ($\boldsymbol{F}_{CO_2}$) are 9.24% (−5.36%), −7.54% (4.59%), and 14.37% (−11.66%), respectively.

5. Conclusions

To understand the features of breeze events and their impacts on energy fluxes and carbon dioxide exchange in mountainous lake areas, an investigation into the relationship between breeze events and turbulence anomalies was conducted based on ECMWF reanalysis data, meteorological observations, and EC observation data from the Dali Basin,

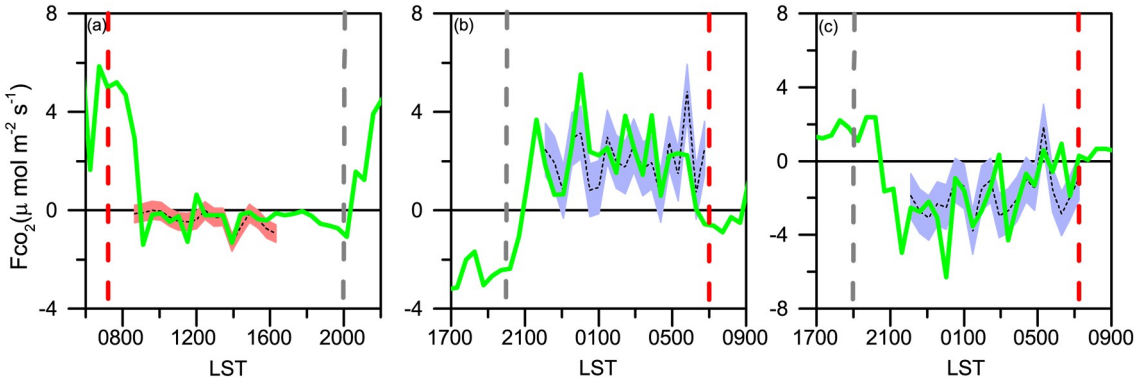

Fig. 11. F_{CO_2} anomalies for (a) an example daytime breeze event (11/08/2015), (b) an example N1 breeze event (12/08/2015), and (c) an example N2 breeze event (24/10/2015) at the EC site are indicated with green lines. The vertical gray (red) solid lines indicate sunset (sunrise). The F_{CO_2} anomaly mean for all events is shown with black dots, and the standard deviation is shown with shadow.

southwest China. This study focuses on comparisons between different types of breeze events and the effects they each have on sensible heat flux, latent heat flux and carbon dioxide flux exchange over complex terrain.

Influenced by the Cangshan Mountain range and Erhai Lake, the locality at the Dali Basin is characterized by a combination of mountain–valley and lake–land breeze circulations, leading to extended lake breezes. To analyze these extended lake breezes systematically, three types of breeze events (daytime, N1, and N2) are defined according to Arrillaga et al. (2016) and Román-Cascón et al. (2019). Due to the interactions between the mountain breeze and the land breeze, nighttime events have been divided into two types (N1 and N2 breeze events). At the EC site, daytime breeze events occur more frequently than nighttime breeze events. The number of detected daytime, and N1 and N2 nighttime breeze events is 149, 22, and 112, respectively. Daytime and N2 breeze events are dominated by the southeast wind, while N1 breeze events are mainly dominated by the west wind. Wind speed of daytime breeze events is slightly higher than N1 events, but lower than N2 events. Since the lake surface is smoother than land surface, wind speed is higher when it blows from the lake.

Nighttime breeze events last longer than daytime events. Event duration is controlled mainly by sunlight hours and the development of local circulation. The lake breeze usually forms 1–2 hours after sunrise, and then daytime breeze events begin. With the decay and disappearance of the lake breeze circulation, daytime breeze events end a few hours before the evening transition. With the arrival of the mountain breeze, N1 nighttime breeze events generally start around 1.5 hours before sunset. N2 breeze events begin during evening transition or half an hour later with the assistance of cyclonic circulation in the southern part of the lake.

The influence of daytime and nighttime breeze events on energy and carbon dioxide exchange processes at the Dali Basin has also been analyzed. Daytime breeze events decrease Hs by an average of 6.5 W m^{-2}. N1 breeze events reduce Hs by an average of 15.1 W m^{-2}, while N2 events increase Hs by 12.4 W m^{-2}. The LE anomaly is positive during daytime breeze events. Coinciding with large wind speeds and wet air masses, the lake breeze increases LE exchange by 38.2 W m^{-2}. For N1 events, the mountain breeze decreases LE by 46.6 W m^{-2}. With the assistance of the southeast wind from the lake surface, N2 events increase Hs by 58.3 W m^{-2}. The lake decreases F_{CO_2} by 0.4 μ mol m^{-2} s^{-1} and 1.8 μ mol m^{-2} s^{-1}, respectively, for daytime and N2 events. However, for N1 events, it has a positive effect of 2.1 μ mol m^{-2} s^{-1}.

These results demonstrate several unique features of daytime and nighttime breeze events at the Dali basin based on one year's dataset. Longer data recording would be helpful to quantify the general characteristics of breeze events in this mountainous lake area. Moreover, field experiments in the horizontal and vertical direction are needed to further investigate energy and carbon dioxide exchange at different temporal and spatial scales. The role of advection and convection in turbulence and carbon transportation will be investigated in future studies.

Acknowledgements. This study was supported by funds from the National Key Research and Development Program of China (Project no: 2017YFC1502101) and the National Natural Science Foundation of China (Projects no: 41775018, and 41805010).

REFERENCES

Alcott, T. I., W. J. Steenburgh, and N. F. Laird, 2012: Great Salt Lake–effect precipitation: Observed frequency, characteristics, and associated environmental factors. *Wea. Forecasting*, **27**(4), 954–971, https://doi.org/10.1175/waf-d-12-00016.1.

Arrillaga, J. A., C. Yagüe, M. Sastre, and C. Román-Cascón, 2016: A characterisation of sea-breeze events in the eastern Cantabrian coast (Spain) from observational data and WRF simulations. *Atmospheric Research*, **181**, 265–280, https://doi.org/10.1016/j.atmosres.2016.06.021.

Arrillaga, J. A., C. Yagüe, C. Román-Cascón, M. Sastre, M. A. Jiménez, G. Maqueda, and J. V. G. de Arellano, 2019: From

weak to intense downslope winds: Origin, interaction with boundary-layer turbulence and impact on CO_2 variability. *Atmospheric Chemistry and Physics*, **19**(7), 4615–4635, https://doi.org/10.5194/acp-19-4615-2019.

Arrillaga, J. A., J. V. G. de Arellano, F. Bosveld, H. K. Baltink, C. Yagüe, M. Sastre, and C. Román-Cascón, 2018: Impacts of afternoon and evening sea-breeze fronts on local turbulence, and on CO_2 and radon-222 transport. *Quart. J. Roy. Meteor. Soc.*, **144**(713), 990–1011, https://doi.org/10.1002/qj.3252.

Bartůňkova, K., Z. Sokol, and L. Pop, 2014: Simulations of the influence of lake area on local temperature with the COSMO NWP model. *Atmospheric Research*, **147-148**, 51–67, https://doi.org/10.1016/j.atmosres.2014.05.003.

Bergström, H., and N. Juuso, 2006: A study of valley winds using the MIUU meso-scale model. *Wind Energy*, **9**(1), 109–129, https://doi.org/10.1002/we.188.

Biermann, T., W. Babel, W. Q. Ma, X. L. Chen, E. Thiem, Y. M. Ma, and T. Foken, 2014: Turbulent flux observations and modelling over a shallow lake and a wet grassland in the Nam Co basin, Tibetan Plateau. *Theor. Appl. Climatol.*, **116**, 301–316, https://doi.org/10.1007/s00704-013-0953-6.

Bischoff-Gauß, I., N. Kalthoff, and M. Fiebig-Wittmaack, 2006: The influence of a storage lake in the Arid Elqui Valley in Chile on local climate. *Theor. Appl. Climatol.*, **85**, 227–241, https://doi.org/10.1007/s00704-005-0190-8.

Borges, A. V., C. Morana, S. Bouillon, P. Servais, J. P. Descy, and F. Darchambeau, 2014: Carbon cycling of Lake Kivu (East Africa): Net autotrophy in the epilimnion and emission of CO_2 to the atmosphere sustained by geogenic inputs. *PLoS One*, **9**(10), e109500, https://doi.org/10.1371/journal.pone.0109500.

Boybeyi, Z., and S. Raman, 1992: A three-dimensional numerical sensitivity study of mesoscale circulations induced by circular lakes. *Meteorol. Atmos. Phys.*, **49**, 19–41, https://doi.org/10.1007/BF01025399.

Crosman, E. T., and J. D. Horel, 2012: Idealized large-eddy simulations of Sea and Lake Breezes: Sensitivity to lake diameter, heat flux and stability. *Bound.-Layer Meteorol.*, **144**, 309–328, https://doi.org/10.1007/s10546-012-9721-x.

Crosman, E. T., and J. D. Horel, 2016: Winter lake breezes near the Great Salt Lake. *Bound.-Layer Meteorol.*, **159**(2), 439–464, https://doi.org/10.1007/s10546-015-0117-6.

Curry, M., J. Hanesiak, and D. Sills, 2015: A radar-based investigation of lake breezes in southern Manitoba, Canada. *Atmosphere-Ocean*, **53**(2), 237–250, https://doi.org/10.1080/07055900.2014.1001317.

Curry, M., J. Hanesiak, S. Kehler, D. M. L. Sills and N. M. Taylor, 2017: Ground-based observations of the thermodynamic and kinematic properties of lake-breeze fronts in southern Manitoba, Canada. *Bound.-Layer Meteorol.*, **163**(1), 143–159, https://doi.org/10.1007/s10546-016-0214-1.

Davis, Z. Y. W., D. M. L. Sills, and R. McLaren, 2020: Enhanced NO_2 and aerosol extinction observed in the tropospheric column behind lake-breeze fronts using MAX-DOAS. *Atmos. Environ.*, **5**, 100066, https://doi.org/10.1016/j.aeaoa.2020.100066.

Du, Q., H. Z. Liu, L. J. Xu, Y. Liu, and L. Wang, 2018a: The monsoon effect on energy and carbon exchange processes over a highland lake in the Southwest of China. *Atmospheric Chemistry and Physics*, **18**, 15 087–15 104, https://doi.org/10.5194/acp-18-15087-2018.

Du, Q., H. Z. Liu, Y. Liu, L. Wang, L. J. Xu, J. H. Sun, and A. L. Xu, 2018b: Factors controlling evaporation and the CO_2 flux over an open water lake in southwest of China on multiple temporal scales. *International Journal of Climatology*, **38**(13), 4723–4739, https://doi.org/10.1002/joc.5692.

Ezber, Y., O. L. Sen, Z. Boybeyi, and M. Karaca, 2015: Investigation of local flow features in Istanbul. Part I: High-resolution sensitivity simulations. *International Journal of Climatology*, **35**(13), 3812–3833, https://doi.org/10.1002/joc.4248.

Feng, J. W., H. Z. Liu, J. H. Sun, and L. Wang, 2016: The surface energy budget and interannual variation of the annual total evaporation over a highland lake in Southwest China. *Theor. Appl. Climatol.*, **126**(1–2), 303–312, https://doi.org/10.1007/s00704-015-1585-9.

Fernando, H. J. S., and Coauthors, 2015: The MATERHORN: Unraveling the intricacies of mountain weather. *Bull. Amer. Meteor. Soc.*, **96**(11), 1945–1967, https://doi.org/10.1175/BAMS-D-13-00131.1.

Filonov, A., I. Tereshchenko, J. Alcocer, and C. Monzón, 2015: Dynamics of internal waves generated by mountain breeze in Alchichica Crater Lake, Mexico. *Geofisica Internacional*, **54**(1), 21–30, https://doi.org/10.1016/j.gi.2015.04.001.

Foken, T., M. Göockede, M. Mauder, L. Mahrt, B. Amiro, and W. Munger, 2004: Post-field data quality control. *Handbook of Micrometeorology: A Guide for Surface Flux Measurement and Analysis*, X. Lee, W. Massman, and B. Law, Eds., Kluwer Academic Publishers, https://doi.org/10.1007/1-4020-2265-4_9.

Ganbat, G., and J. J. Baik, 2015: Local circulations in and around the Ulaanbaatar, Mongolia, metropolitan area. *Meteorol. Atmos. Phys.*, **127**(4), 393–406, https://doi.org/10.1007/s00703-015-0374-4.

Gerken, T., W. Babel, F. L. Sun, M. Herzog, Y. M. Ma, T. Foken, and H.-F. Graf, 2013: Uncertainty in atmospheric profiles and its impact on modeled convection development at Nam Co Lake, Tibetan Plateau. *J. Geophys. Res.*, **118**(22), 12 317–12 331, https://doi.org/10.1002/2013jd020647.

Gerken, T., T. Biermann, W. Babel, M. Herzog, Y. M. Ma, T. Foken, and H.-F. Graf, 2014: A modelling investigation into lake-breeze development and convection triggering in the Nam Co Lake basin, Tibetan Plateau. *Theor. Appl. Climatol.*, **117**, 149–167, https://doi.org/10.1007/s00704-013-0987-9.

Giovannini, L., L. Laiti, D. Zardi, and M. De Franceschi, 2015: Climatological characteristics of the Ora del Garda wind in the Alps. *International Journal of Climatology*, **35**(14), 4103–4115, https://doi.org/10.1002/joc.4270.

Guo, Y. H., Y. S. Zhang, N. Ma, J. Q. Xu, and T. Zhang, 2019: Long-term changes in evaporation over Siling Co Lake on the Tibetan Plateau and its impact on recent rapid lake expansion. *Atmospheric Research*, **216**, 141–150, https://doi.org/10.1016/j.atmosres.2018.10.006.

Hai, P., R. Avissar, and D. B. Haidvogel, 2002: Summer circulation and temperature structure of Lake Kinneret. *J. Phys. Oceanogr.*, **32**(1), 295–313, https://doi.org/10.1175/1520-0485(2002)032<0295:SCATSO>2.0.CO;2.

Han, B., and Coauthors, 2020: Connections between daily surface temperature contrast and CO_2 flux over a Tibetan Lake: A case study of Ngoring Lake. *J. Geophys. Res.*, **125**, e2019JD032277, https://doi.org/10.1029/2019JD032277.

Harris, L., and V. R. Kotamarthi, 2005: The characteristics of the Chicago Lake Breeze and its effects on trace particle trans-

port: Results from an episodic event simulation. *J. Appl. Meteorol.*, **44**(11), 1637–1654, https://doi.org/10.1175/JAM2301.1.

Jeppesen, E., and Coauthors, 2016: Major changes in CO_2 efflux when shallow lakes shift from a turbid to a clear water state. *Hydrobiologia*, **778**(1), 33–44, https://doi.org/10.1007/s10750-015-2469-9.

Jiménez, M. A., and J. Cuxart, 2014: A study of the nocturnal flows generated in the north side of the Pyrenees. *Atmospheric Research*, **145–146**, 244–254, https://doi.org/10.1016/j.atmosres.2014.04.010.

Kaimal, J. C., and Finnigan J. J., 1994: *Atmospheric Boundary Layer Flows: Their Structure and Measurement*. Oxford University Press.

Kondo, H., 1990: A numerical experiment on the interaction between sea breeze and valley wind to generate the so-called "Extended Sea Breeze". *J. Meteor. Soc. Japan*, **68**, 435–446, https://doi.org/10.2151/jmsj1965.68.4_435.

Kossmann, M., A. P. Sturman, P. Zawar-Reza, H. A. McGowan, A. J. Oliphant, I. F. Owens, and R. A. Spronken-Smith, 2002: Analysis of the wind field and heat budget in an alpine lake basin during summertime fair weather conditions. *Meteorol. Atmos. Phys.*, **81**, 27–52, https://doi.org/10.1007/s007030200029.

Laiti, L., D. Zardi, M. De Franceschi, and G. Rampanelli, 2013a: Analysis of the diurnal development of the Ora del Garda wind in the Alps from airborne and surface measurements. *Atmospheric Chemistry and Physics*, **13**(7), 19 121–19 171, https://doi.org/10.5194/acpd-13-19121-2013.

Laiti, L., D. Zardi, M. De Franceschi, and G. Rampanelli, 2013b: Atmospheric boundary layer structures associated with the Ora del Garda wind in the Alps as revealed from airborne and surface measurements. *Atmospheric Research*, **132–133**, 473–489, https://doi.org/10.1016/j.atmosres.2013.07.006.

Laiti, L., D. Zardi, M. De Franceschi, G. Rampanelli, and L. Giovannini, 2014: Analysis of the diurnal development of a lake-valley circulation in the Alps based on airborne and surface measurements. *Atmospheric Chemistry and Physics*, **14**, 9771–9786, https://doi.org/10.5194/acp-14-9771-2014.

Lehner, M., and M. W. Rotach, 2018: Current challenges in understanding and predicting transport and exchange in the atmosphere over mountainous Terrain. *Atmosphere*, **9**(7), 276, https://doi.org/10.3390/atmos9070276.

Li, E. H., X. L. Wang, X. B. Cai, X. Y. Wang, and S. T. Zhao, 2011: Features of aquatic vegetation and the influence factors in Erhai lakeshore wetland. *Journal of Lake Sciences*, **23**(5), 738–746, https://doi.org/10.18307/2011.0511. (in Chinese with English abstract)

Lin, J. C., and Coauthors, 2018: CO_2 and carbon emissions from cities: Linkages to air quality, socioeconomic activity, and stakeholders in the Salt Lake City urban area. *Bull. Amer. Meteor. Soc.*, **99**(11), 2325–2339, https://doi.org/10.1175/bams-d-17-0037.1.

Liu, H. Z., J. W. Feng, J. H. Sun, L. Wang, and A. L. Xu, 2015: Eddy covariance measurements of water vapor and CO_2 fluxes above the Erhai Lake. *Science China Earth Sciences*, **58**(3), 317–328, https://doi.org/10.1007/s11430-014-4828-1.

Mahrt, L., 2017: Stably stratified flow in a shallow valley. *Bound.-Layer Meteorol.*, **162**(1), 1–20, https://doi.org/10.1007/s10546-016-0191-4.

McGowan, H. A., I. Owens, and A. P. Sturman, 1995: Thermal and dynamic characteristics of alpine lake breezes, Lake Tekapo, New Zealand. *Bound.-Layer Meteorol.*, **76**, 3–24, https://doi.org/10.1007/BF00710888.

Mengelkamp, H. T., and Coauthors, 2006: Evaporation over a heterogeneous land surface-The EVA-GRIPS project. *Bull. Amer. Meteor. Soc.*, **87**(6), 775–786, https://doi.org/10.1175/BAMS-87-6-775.

Moore, C. J., 1986: Frequency response corrections for eddy correlation systems. *Bound.-Layer Meteorol.*, **37**, 17–35, https://doi.org/10.1007/BF00122754.

Naor, R., O. Potchter, H. Shafir, and P. Alpert, 2017: An observational study of the summer Mediterranean Sea breeze front penetration into the complex topography of the Jordan Rift Valley. *Theor. Appl. Climatol.*, **127**(1), 275–284, https://doi.org/10.1007/s00704-015-1635-3.

Nordbo, A., S. Launiainen, I. Mammarella, M. Leppäranta, J. Huotari, A. Ojala, and T. Vesala, 2011: Long-term energy flux measurements and energy balance over a small boreal lake using eddy covariance technique. *J. Geophys. Res.*, **116**(D2), D02119, https://doi.org/10.1029/2010JD014542.

Pérez-Landa, G. and Coauthors, 2007a: Mesoscale circulations over complex terrain in the Valencia coastal region, Spain-Part 2: Modeling CO_2 transport using idealized surface fluxes. *Atmospheric Chemistry and Physics*, **7**(7), 1851–1868, https://doi.org/10.5194/acp-7-1851-2007.

Pérez-Landa, G., P. Ciais, M. J. Sanz, B. Gioli, F. Miglietta, J. L. Palau, G. Gangoiti, and M. M. Millán, 2007b: Mesoscale circulations over complex terrain in the Valencia coastal region, Spain - Part 1: Simulation of diurnal circulation regimes. *Atmospheric Chemistry and Physics*, **7**(7), 1835–1849, https://doi.org/10.5194/acp-7-1835-2007.

Pu, Z. X., C. N. Chachere, S. W. Hoch, E. Pardyjak, and I. Gultepe, 2016: Numerical prediction of cold season fog events over complex terrain: The performance of the WRF Model During MATERHORN-Fog and Early evaluation. *Pure Appl. Geophys.*, **173**(9), 3165–3186, https://doi.org/10.1007/s00024-016-1375-z.

Román-Cascón, C., and Coauthors, 2019: Comparing mountain breezes and their impacts on CO_2 mixing ratios at three contrasting areas. *Atmospheric Research*, **221**, 111–126, https://doi.org/10.1016/j.atmosres.2019.01.019.

Rotach, M. W., and Coauthors, 2016: Investigating exchange processes over complex topography: The Innsbruck Box (i-Box). *Bull. Amer. Meteor. Soc.*, **98**(4), 787–805, https://doi.org/10.1175/BAMS-D-15-00246.1.

Segal, M., M. Leuthold, R. W. Arritt, C. Anderson, and J. Shen, 2010: Small lake daytime breezes: Some observational and conceptual evaluations. *Bull. Amer. Meteor. Soc.*, **78**, 1135–1148, https://doi.org/10.1175/1520-0477(1997)078<1135:SLDBSO>2.0.CO;2.

Serafin, S., and Coauthors, 2018: Exchange processes in the atmospheric boundary layer over mountainous terrain. *Atmosphere*, **9**(3), 102, https://doi.org/10.3390/atmos9030102.

Sturman, A. P., and Coauthors, 2003: The Lake Tekapo Experiment (LTEX): An investigation of atmospheric boundary layer processes in complex terrain. *Bull. Amer. Meteorol. Soc.*, **84**(3), 371–380, https://doi.org/10.1175/BAMS-84-3-371.

Sun, J. L., and Coauthors, 1997: Lake - induced atmospheric circulations during BOREAS. *J. Geophys. Res.*, **102**(D24), 29 155–29 166, https://doi.org/10.1029/97JD01114.

Tian, Y., and J. F. Miao, 2019: Overview of mountain-valley breeze studies in China. *Meteorological Science and Techno-*

logy, **47**(1), 41–51, https://doi.org/10.19517/j.1671-6345.20170777. (in Chinese with English abstract)

Verpoorter, C., T. Kutser, D. A. Seekell, and L. J. Tranvik, 2014: A global inventory of lakes based on high-resolution satellite imagery. *Geophys. Res. Lett.*, **41**(18), 6396–6402, https://doi.org/10.1002/2014gl060641.

Vickers, D., and L. Mahrt, 1997: Quality control and flux sampling problems for tower and aircraft data. *J. Atmos. Ocean. Technol.*, **14**(3), 512–526, https://doi.org/10.1175/1520-0426(1997)014<0512:QCAFSP>2.0.CO;2.

Wagner-Riddle, C., S. S. Werner, P. Caramori, W. S. Ricce, P. Nitsche, P. von Bertoldi, and E. F. De Souza, 2015: Determining the influence of Itaipu Lake on thermal conditions for soybean development in adjacent lands. *International Journal of Biometeorology*, **59**(10), 1499–1509, https://doi.org/10.1007/s00484-015-0960-7.

Wang, Y. W., and Coauthors, 2017: Spatiotemporal characteristics of lake breezes over Lake Taihu, China. *J. Appl. Meteor. Climatol.*, **56**(7), 2053–2065, https://doi.org/10.1175/JAMC-D-16-0220.1.

Webb, E. K., G. I. Pearman, and R. Leuning, 1980: Correction of flux measurements for density effects due to heat and water vapour transfer. *Quart. J. Roy. Meteorol. Soc.*, **106**(447), 85–100, https://doi.org/10.1002/qj.49710644707.

Williamson, C. E., J. E. Saros, W. F. Vincent, and J. P. Smol, 2009: Lakes and reservoirs as sentinels, integrators, and regulators of climate change. *Limnology and Oceanography*, **54**(6), 2273–2282, https://doi.org/10.4319/lo.2009.54.6_part_2.2273.

Xu, J. Q., S. M. Yu, J. S. Liu, S. Haginoya, Y. Ishigooka, T. Kuwagata, M. Hara, and T. Yasunari, 2009: The Implication of Heat and Water Balance Changes in a Lake Basin on the Tibetan Plateau. *Hydrological Research Letters*, **3**, 1–5, https://doi.org/10.3178/hrl.3.1.

Xu, L. J., and H. Z. Liu, 2015: Numerical simulation of the lake effect of Erhai in the Yunnan-Guizhou Plateau Area. *Acta Meteorologica Sinica*, **73**(4), 789–802, https://doi.org/10.11676/qxxb2015.047. (in Chinese with English abstract)

Xu, L. J., H. Z. Liu, Q. Du, and L. Wang, 2016: Evaluation of the WRF-lake model over a highland freshwater lake in Southwest China. *J. Geophys. Res.*, **121**(23), 13 989–14 005, https://doi.org/10.1002/2016JD025396.

Xu, L. J., H. Z. Liu, Q. Du, L. Wang, L. Yang, and J. H. Sun, 2019: Differences of atmospheric boundary layer characteristics between pre-monsoon and monsoon period over the Erhai Lake. *Theor. Appl. Climatol.*, **135**(1), 305–321, https://doi.org/10.1007/s00704-018-2386-8.

Zumpfe, D. E., and J. D. Horel, 2007: Lake-breeze fronts in the Salt Lake Valley. *J. Appl. Meteor. Climatol.*, **46**(2), 196–211, https://doi.org/10.1175/JAM2449.1.